Krzysztof MAKOWSKI, Marcin J. WILK

Wroclaw University of Technology, Institute of Electrical Machines, Drives and Measurements

Determination of dynamic characteristics of the single-phase capacitor induction motor

Abstract. *The paper presents a mathematical model and simulation results of dynamic characteristics of the single-phase capacitor induction motor for different values of the capacitor capacitance and moment of inertia at no-load and nominal load conditions. The model has been used to study the effect of some machine parameters on the start-up and load performance of the motor. Computed dynamic characteristics were compared with measured ones to confirm correctness of the mathematical model and parameters.*

Streszczenie. *Artykuł przedstawia model matematyczny oraz wyniki symulacji stanów dynamicznych jednofazowego silnika indukcyjnego z pomocniczym uzwojeniem kondensatorowym dla różnych pojemności kondensatora pracy oraz momentu bezwładności. Obliczone charakterystyki dynamiczne porównano z wynikami eksperymentalnymi dla sprawdzenia poprawności modelu matematycznego i przyjętych parametrów.* ***Wyznaczanie charakterystyk dynamicznych jednofazowego silnika indukcyjnego z pomocniczym uzwojeniem kondensatorowym.***

Keywords: small-power induction motor, single-phase, run capacitor, circuit modelling.
Słowa kluczowe: silniki indukcyjne małej mocy, jednofazowe, kondensator pracy, modelowanie obwodowe

Introduction

Single-phase capacitor induction motors (SPCIMs) are commonly used as a drive for fans, pumps and compressors. Generally, they are induction machines of the symmetrical rotor cage and non-symmetrical two stator windings (the main winding and auxiliary winding with starting or running capacitor) supplied with the same sinusoidal voltage source. In modelling performance characteristics of the induction motors circuit models of lumped parameters are still often used due to their simplicity and fast computation. At first approximation of the mathematical models linearity of magnetic circuit is assumed and slotting of the stator and rotor are neglected [1-3]. Majority of SPCIM models for analysis of performance of the motor with variety variants of winding-capacitor arrangements referred in literature have used two-axis models or based on rotating magnetic field theory models that include higher mmf harmonics. Authors in the paper [4] presented a general model the permanent split capacitor induction machine of asymmetrical windings and arbitrary tapping of the main winding with the auxiliary winding. The model was validated by experimental results obtained at steady-state performance of the tested motor. In the paper [5] a simplified equivalent circuit model was proposed which have been used for calculating steady-state characteristics for various values of capacitor capacitance and phase angle difference. Experimental study of an influence of stator winding harmonics on torque-speed characteristics were presented in [6] which shown considerable impact of the harmonics on the starting performance of the motor. Authors in [7] presented the concept of equivalent circuit which parameters were determined by finite element method. Dynamic analysis of the SPCIM were also studied in [8]. General equations of a single-phase induction motor in dq system and their application for simulation at continuously varied capacitance to improve performance of the motor were presented. In the paper [9] only simulation of currents, electromagnetic torque and voltage across capacitor of the motor using PSPICE and EMTP packages were presented without velocity waveforms and comparison of the electromagnetic torque with an experiment. These models may be completely useful for preliminary or initial searching of better structural solutions in design optimization.

In the paper the mathematical model of the capacitor induction motor in the stationary dq system is described and developed for simulation start-up of the motor at no-load and application of nominal load torque after starting from no-load operation. The mathematical model and parameters of the capacitor motor in the dq system for steady-state operation is described in details in [10, 11, 12]. The simulations include waveforms and steady-state characteristics of the tested capacitor induction motor for different values of capacitor capacitance placed in the auxiliary stator winding.

Description of mathematical model of SPCIM

The single-phase 2 poles capacitor induction motor which cross-section and the *dq* model are shown in Fig. 1 was used for computational analysis. The main (M) and auxiliary (A) stator windings are distributed in stator slots so that they form the *dq* axes fields. The capacitor capacitance is placed in the stator auxiliary winding.

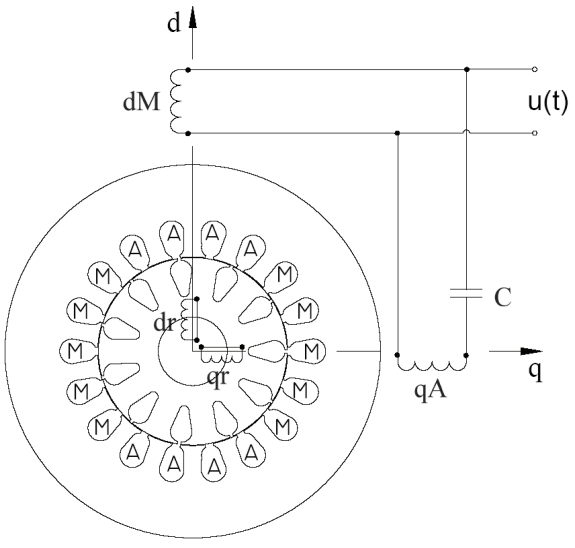

Fig. 1. Cross-section view and the *d-q* model of tested capacitor induction motor

The rotor has squirrel cage of 11 bars uniformly distributed along circumference. The ratings and structural data of the tested motor are listed in Table. 1.

Table 1. Ratings and data of the tested capacitor induction motor

Rated power	0.09 kW
Rated voltage	230 V
Rated current	0.9 A
Rated speed	2840 rev/min
Efficiency	0.55
Power factor	0.9
Frequency	50 Hz
Torque ratio	1.5
Number of stator windings	2
Running capacitor capacitance	3μF
Connection of stator windings	parallel
Number of poles: main/auxiliary winding	2/2
Winding layout: main/auxiliary winding	single layer
Rotor winding	squirrel cage
Number of slots: stator/rotor	18/11
Lamination material - generator sheet	M 600-50A
Laminated core length	32 mm

The mathematical model of the capacitor induction motor can be described by electrical and mechanical differential equations in the arbitrary reference frames as follows:

(1)

$$\frac{di_{dM}}{dt}=\frac{1}{L_{\Sigma}}\left[i_{dM}L'_{rr}R_s+i_{qA}\left(-L_{ms}{}^2(\omega-\omega_r)+L'_{rr}L_{ss}\omega\right)-\right.$$
$$\left.-i'_{dr}R'_rL_{ms}+i'_{qr}L'_{rr}L_{ms}\omega_r-L'_{rr}u_{dM}+u'_{dr}L_{ms}\right]$$

$$\frac{di_{qA}}{dt}=\frac{1}{L_{\Sigma}}\left[i_{dM}\left(L_{ms}{}^2(\omega-\omega_r)-L'_{rr}L_{ss}\omega\right)+i_{qA}L'_{rr}R_s-\right.$$
$$\left.-i'_{dr}L'_{rr}L_{ms}\omega_r-i'_{qr}R'_rL_{ms}-L'_{rr}u_{qA}+u'_{qr}L_{ms}+u_{qC}L'_{rr}\right]$$

$$\frac{di'_{dr}}{dt}=\frac{1}{L_{\Sigma}}\left[-i_{dM}R_sL_{ms}-i_{qA}L_{ss}L_{ms}\omega_r+i'_{dr}R'_rL_{ss}+\right.$$
$$\left.+i'_{qr}\left(L'_{rr}L_{ss}(\omega-\omega_r)-L_{ms}{}^2\omega\right)-u'_{dr}L_{ss}+u_{dM}L_{ms}\right]$$

$$\frac{di'_{qr}}{dt}=\frac{1}{L_{\Sigma}}\left[i_{dM}L_{ss}L_{ms}\omega_r-i_{qA}R_sL_{ms}+i'_{dr}\left(-L'_{rr}L_{ss}(\omega-\omega_r)+L_{ms}{}^2\omega\right)\right.$$
$$\left.+i'_{qr}R'_rL_{ss}-u'_{qr}L_{ss}+u_{qA}L_{ms}-u_{qC}L_{ms}\right]$$

$$\frac{du_{qC}}{dt}=\frac{1}{C}i_{qA}$$

$$\frac{d\omega_r}{dt}=\frac{p^2}{J}L_{ms}\left(i_{dM}i'_{qr}-i_{qA}i'_{dr}\right)-\frac{D_f}{J}\omega_r-\frac{p}{J}T_L$$

$$\frac{d\theta_r}{dt}=\omega_r$$

where:

$$L_{\Sigma}=L_{ms}{}^2-L'_{rr}L_{ss},\ R_s=R_M=R'_A,\ L_{ss}=L_{sM}=L'_{sA}$$

and i_{dM}, i_{qA} are the direct- and quadrature- components of stator currents, i_{dr}, i_{qr} are the direct- and quadrature-components of rotor currents, u_{dM}, u_{qA} are the direct- and quadrature- components of stator voltages, u_{dr}, u_{qr} are the direct- and quadrature- components of rotor voltages, u_{qC} is the voltage across the capacitor, R_s is the resistance of the stator windings, R_r is the resistance of the rotor windings, L_{ss} is the self inductance of the stator windings, L_{rr} is the self inductance of the rotor windings, L_{ms} is the stator magnetizing inductance, p is the number of pole pairs, D_f is the viscous friction coefficient, J is the moment of inertia, T_e is the electromagnetic torque, T_L is the load torque, ω_r is the electrical angular velocity of the rotor, θ_r is the electrical angular displacement of the rotor.

Using the operator s = d/dt and assuming ω=0 dynamic model of the single-phase capacitor induction motor in the stationary reference frames can be build, for which the stator and rotor currents, voltage across the capacitor, angular velocity and angular displacement of the rotor are the state variables:

(2)

$$i_{Md}=\frac{1}{L_{\Sigma}s-L'_{rr}R_s}\left[i_{qA}L_{ms}{}^2\omega_r-i'_{dr}R'_rL_{ms}+i'_{qr}L'_{rr}L_{ms}\omega_r-\right.$$
$$\left.-L'_{rr}u_{dM}+u'_{dr}L_{ms}\right]$$

$$i_{Aq}=\frac{1}{L_{\Sigma}s-L'_{rr}R_s}\left[-i_{dM}L_{ms}{}^2\omega_r-i'_{dr}L'_{rr}L_{ms}\omega_r-i'_{qr}R'_rL_{ms}-\right.$$
$$\left.-L'_{rr}u_{qA}+u'_{qr}L_{ms}+u_{Cq}L'_{rr}\right]$$

$$i'_{dr}=\frac{1}{L_{\Sigma}s-L_{ss}R'_r}\left[-i_{dM}R_sL_{ms}-i_{qA}L_{ss}L_{ms}\omega_r-\right.$$
$$\left.-i'_{qr}L'_{rr}L_{ss}\omega_r-u'_{dr}L_{ss}+u_{dM}L_{ms}\right]$$

$$i'_{qr}=\frac{1}{L_{\Sigma}s-L_{ss}R'_r}\left[i_{dM}L_{ss}L_{ms}\omega_r-i_{qA}R_sL_{ms}+i'_{dr}L'_{rr}L_{ss}\omega_r-\right.$$
$$\left.-u'_{qr}L_{ss}+u_{qA}L_{ms}-u_{qC}L_{ms}\right]$$

$$u_{qC}=\frac{1}{sC}i_{qA}$$

$$\omega_r=p\left(\frac{1}{Js+D_f}\right)\left[pL_{ms}\left(i_{dM}i'_{qr}-i_{qA}i'_{dr}\right)-T_L\right]$$

$$\theta_r=\frac{1}{s}\omega_r$$

After some mathematical transformations the set of the motor equations can be written as follows:

(3)

$$i_{dM}=\frac{L_{ms}}{L_{\Sigma}s-L'_{rr}R_s}\left[-i'_{dr}R'_r+\omega_r\left(i_{qA}L_{ms}+i'_{qr}L'_{rr}\right)-\frac{L'_{rr}}{L_{ms}}u_{dM}\right]$$

$$i_{qA}=\frac{L_{ms}}{L_{\Sigma}s-L'_{rr}R_s}\left[-i'_{qr}R'_r-\omega_r\left(i_{dM}L_{ms}+i'_{dr}L'_{rr}\right)+\frac{L'_{rr}}{L_{ms}}u_{qA}\right]$$

$$i'_{dr}=\frac{1}{L_{\Sigma}s-L_{ss}R'_r}\left[-i_{dM}L_{ms}R_s-\omega_rL_{ss}\left(i_{qA}L_{ms}+i'_{qr}L'_{rr}\right)+L_{ms}u_{dM}\right]$$

$$i'_{qr}=\frac{1}{L_{\Sigma}s-L_{ss}R'_r}\left[-i_{qA}L_{ms}R_s+\omega_rL_{ss}\left(i_{dM}L_{ms}+i'_{dr}L'_{rr}\right)-L_{ms}u_{qA}\right]$$

$$u_{qC}=\frac{1}{sC}i_{qA}$$

$$\omega_r=p\left(\frac{1}{Js+D_f}\right)\left[pL_{ms}\left(i_{dM}i'_{qr}-i_{qA}i'_{dr}\right)-T_L\right]$$

$$\theta_r=\frac{1}{s}\omega_r$$

where:

$$u_{qA}=-\left(u(t)-u_{qC}\right)=-u(t)+u_{qC}$$

$$L_{\Sigma}=L_{ms}{}^2-L'_{rr}L_{ss}$$

Dynamic operation of the tested motor

The dynamic behaviour of the capacitor motor supplied from sinusoidal voltage source of 230V and 50 Hz at different capacitor capacitance was studied for two cases:

- the start-up of the motor with no-load (T_L=0) until steady-state is reached (free acceleration)
- the starting of the motor at no-load and after 0.7s applying the rated load (T_L=T_N) until steady-state is reached.

All simulations were performed at the nominal moment of inertia of the motor (J=0.00007 kgm^2) and the viscous friction coefficient D_f =0.00005 Nms.

Motor starting waveforms obtained at no-load operation are given in Figs. 2-4.

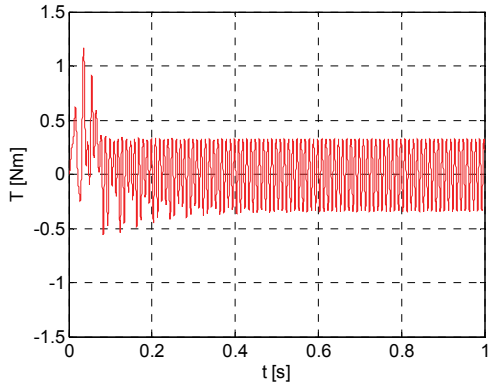

Fig. 2. The electromagnetic torque $T_e(t)$ at no-load: T_{eav}=0.016Nm, T_{em}=0.31Nm

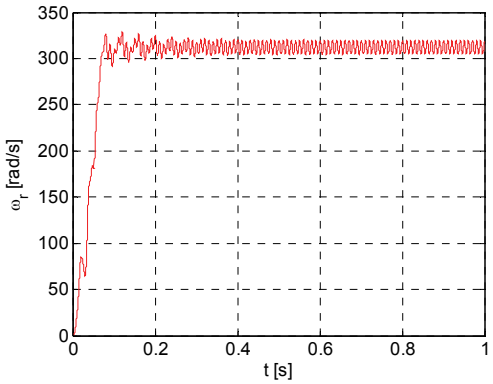

Fig.3. The angular velocity of rotor $\omega_r(t)$ at no-load : ω_{rav}=312 rad/s, ω_{rm}=7.6 rad/s

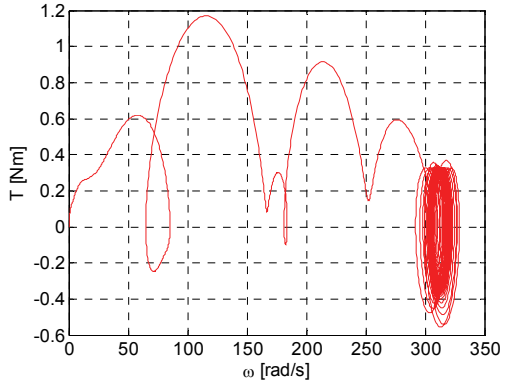

Fig. 4. Torque-speed characteristic at no-load

After the motor is reaching no-load steady-state operation, it can be observed in torque waveform oscillations at twice line frequency which influence on non-uniform running of the rotor (pulsations of the angular velocity). This is the reason of elliptical rotational field in the air-gap due to asymmetry of the stator windings. Phase shift between currents and voltages of the stator windings for no-load and the capacitor capacitance of 3μF are illustrated by the relative current and voltage runs in Figs. 5-6.

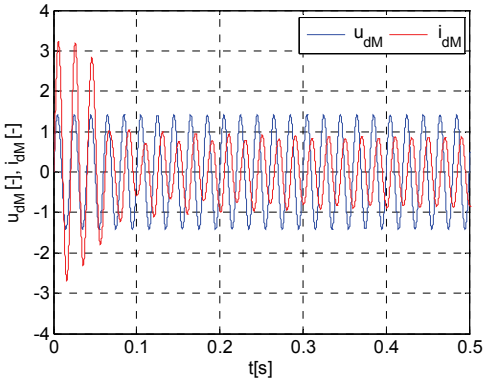

Fig.5. The current/voltage of stator main winding at no-load

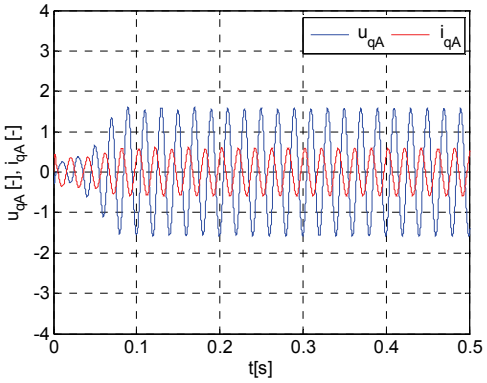

Fig.6. The current/voltage of stator auxiliary winding at no-load

The waveforms of the motor starting from no-load operation and after application of rated load are shown in Figs. 7-11.

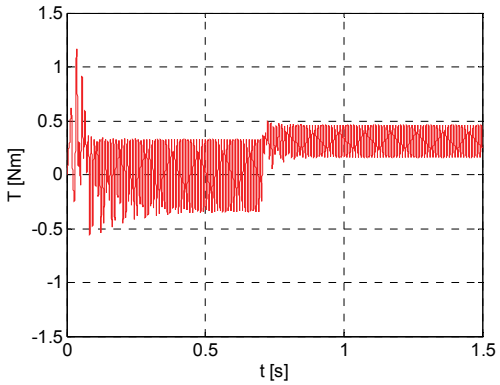

Fig. 7. The electromagnetic torque $T_e(t)$ at rated load: C=3μF T_{eav}=0.314Nm, T_m=0.15Nm

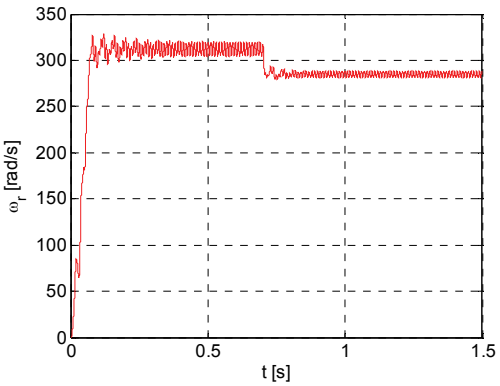

Fig.8. The angular velocity of rotor $\omega_r(t)$ at rated load : C=3μF ω_{rav}=285 rad/s, ω_{rm}=3.4 rad/s

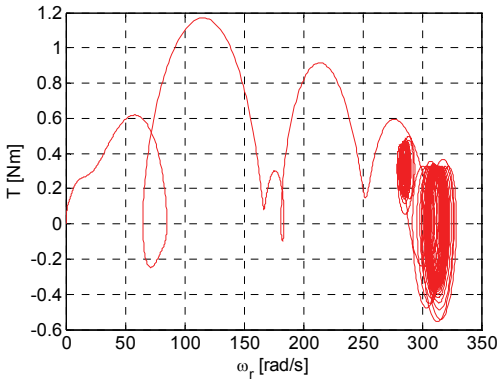

Fig. 9. Torque-speed characteristic at rated load

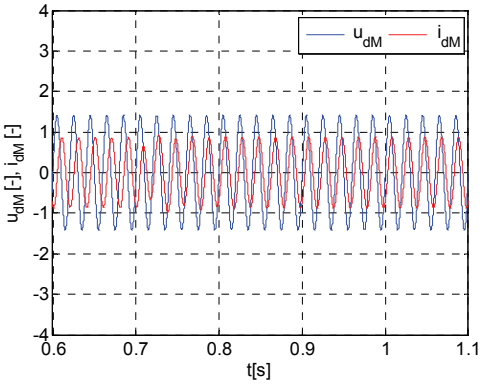

Fig. 10. The current/voltage of stator main winding at rated load

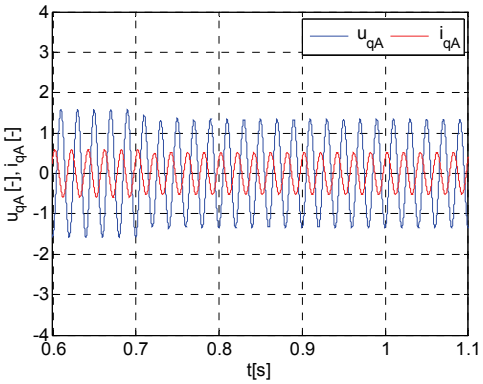

Fig. 11. The current/voltage of stator auxiliary winding at rated load

Influence of capacitor capacitance

Influence of the capacitor capacitance placed within the auxiliary stator winding on amplitude of the torque, start-up time and pulsation of rotor velocity are shown in Figs. 12-15.

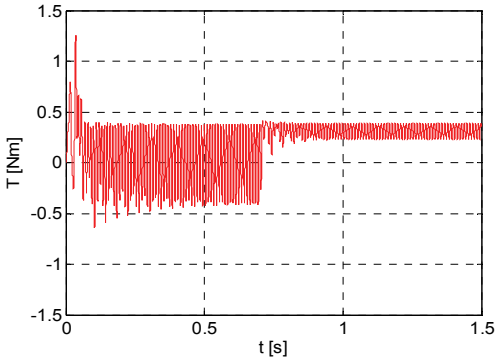

Fig. 12. The electromagnetic torque $T_e(t)$ at rated load: C=4μF, T_{eav}=0.314Nm, T_m=0.081Nm

It is seen that increasing capacitor capacitance up to 4μF causes decreasing electromagnetic torque pulsation and simultaneously increasing start-up time of the motor. Further increase of the capacitance leads to increase of pulsation of the torque. It is evident that the greater capacitor capacitance brings about phase shift increasing between the current and voltage in the auxiliary winding (Figs.14, 15).

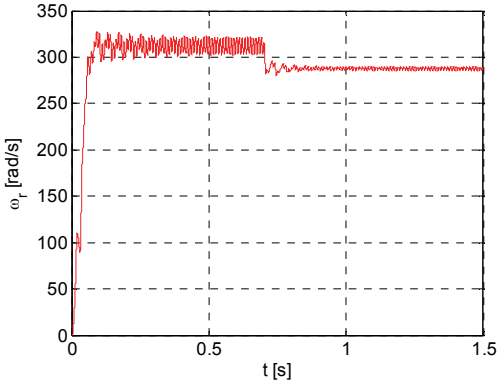

Fig.13. The angular velocity of rotor $\omega_r(t)$ at rated load: C=4μF, ω_{rav}=288 rad/s, ω_{rm}=1.8 rad/s

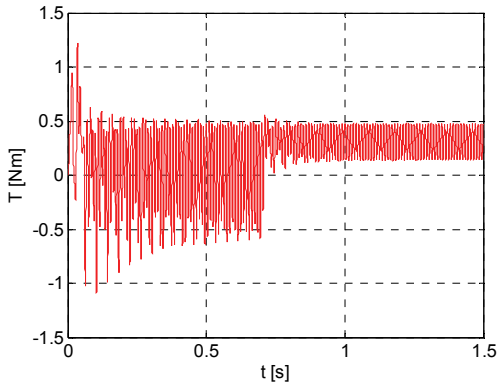

Fig. 14. The electromagnetic torque $T_e(t)$ at rated load: C=5μF, T_{eav}=0.315Nm, T_m=0.17Nm

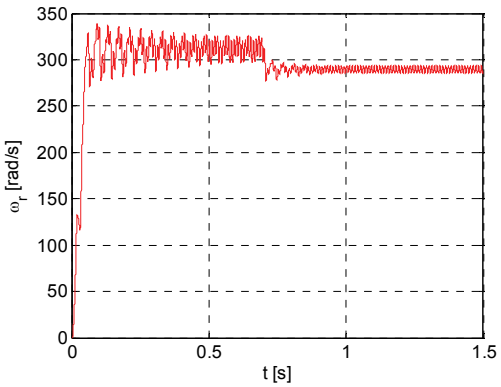

Fig.15. The angular velocity of rotor $\omega_r(t)$ at rated load: C=5μF, ω_{rav}= 288rad/s, ω_{rm}=4 rad/s

It follows that the tested motor has the shortest start-up time and the lowest pulsations of torque and angular velocity at steady-state for capacitor capacitance of 4 μF.

Influence of moment of inertia

An effect of the moment of inertia of the rotor on torque, start-up time and velocity during free acceleration of the motor and after application of rated load are shown in Figs. 16-18 and 21-23.

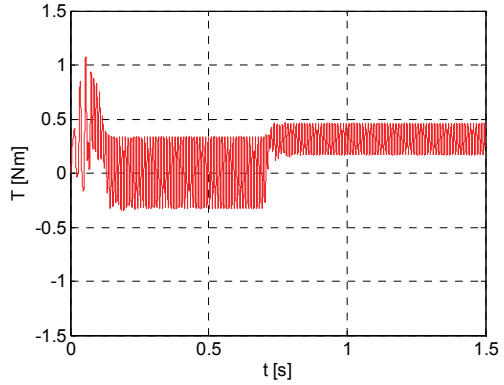

Fig. 16. The electromagnetic torque $T_e(t)$ at rated load: C= 3μF, J=0.00014 kgm^2

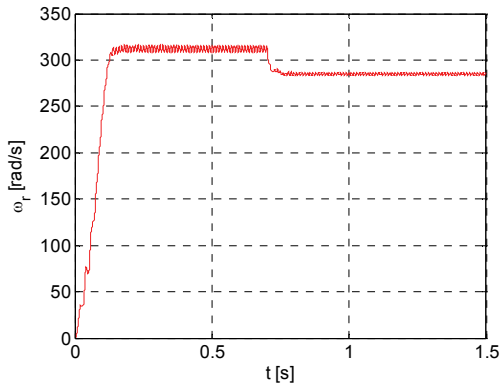

Fig. 17. The angular velocity of rotor $\omega_r(t)$ at rated load: C= 3μF, J=0.00014 kgm^2

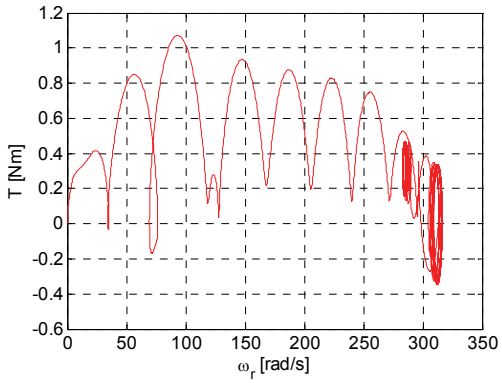

Fig. 18. Torque-speed characteristic at rated load for C= 3μF, J=0.00014 kgm^2

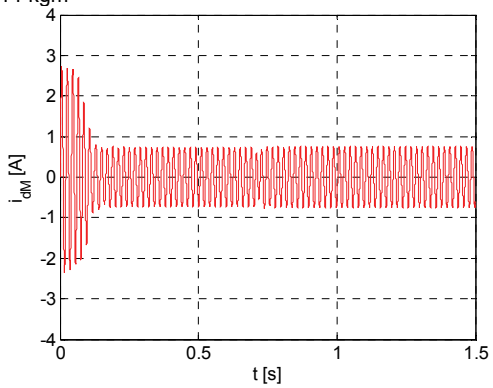

Fig. 19. The current of stator main winding at rated load for C= 3μF, J=0.00014 kgm^2

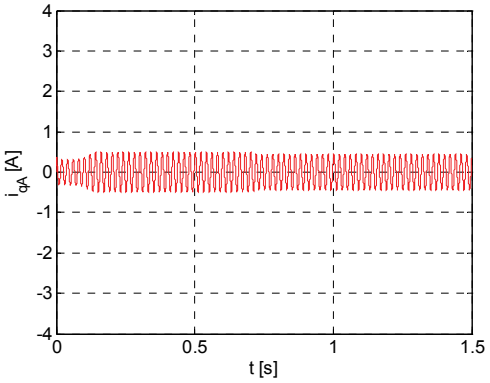

Fig. 20. The current of stator auxiliary winding at rated load for C= 3μF, J=0.00014 kgm^2

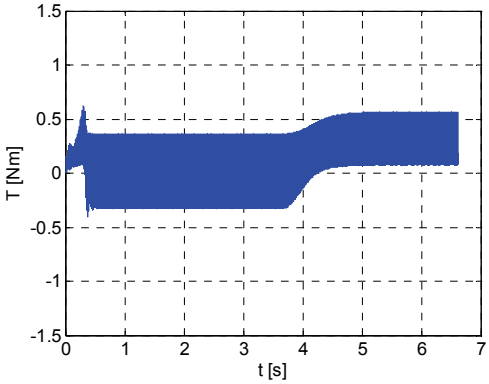

Fig. 21. The electromagnetic torque $T_e(t)$ at rated load: C= 3μF, J=0.00021 kgm^2

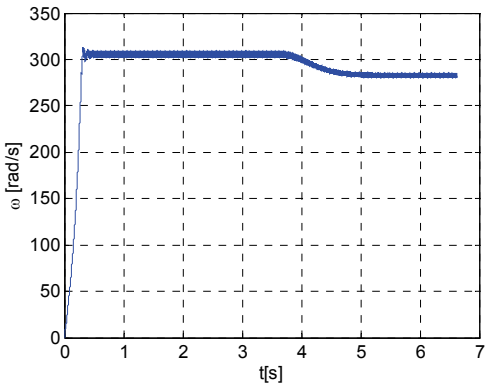

Fig. 22. The angular velocity of rotor $\omega_r(t)$ at rated load: C= 3μF, J=0.00021 kgm^2

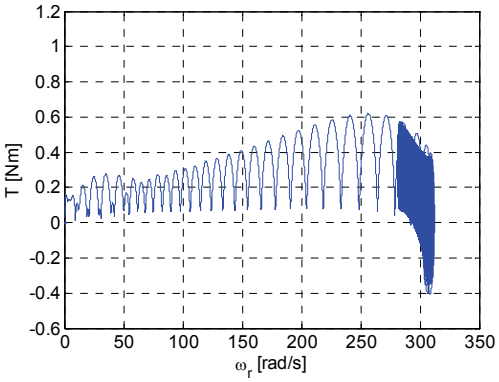

Fig. 23. Torque-speed characteristic at rated load for C= 3μF, J=0.00021 kgm^2

It is evident that the greater moment of inertia causes decreasing pulsations of the electromagnetic torque, rotor velocity and at the same time increasing start-up time of the

motor. After application of load pulsations of the rotor velocity are visibly decreased.

The stator currents waveforms indicate some asymmetry in the main and auxiliary windings for the capacitor capacitance of 3 μF (Figs. 19-20, 24-25).

It is shown by simulation that the lowest pulsations of the torque and velocity at starting occur for the capacitor capacitance of 4μF and further increase of the capacitance leads to increase of the pulsations. On the ground of dynamic simulation it is possible to find an optimal value of the capacitor capacitance which assures desired performance parameters (the start-up time, pulsation of torque and angular velocity) of the capacitor induction motor in transient and steady-state operations.

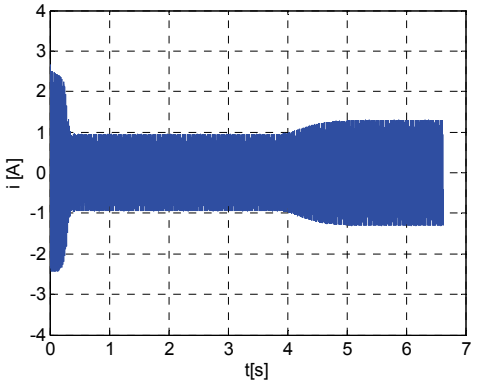

Fig. 24. The intake current at rated load for C= 3μF, J=0.00021 kgm^2

Experimental results

A general scheme of a test bench which was used for measurement of transient characteristics of the tested motor is shown in Fig. 25.

It allows measuring the following electrical and mechanical quantities:

- voltage and intake current of the motor
- rotational speed and torque
- voltage across capacitor

Using the Labview virtual instrument all data for transient waveforms are recorded and then processed by algorithm developed in the Matlab software.

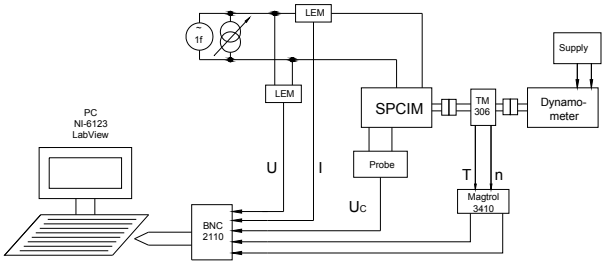

Fig. 25. Scheme of test bench for single-phase capacitor induction motor

Experimental tests were performed at the same load conditions as simulation which results are shown in Figs. 26-29.

Simulating waveforms of torque, velocity and intake current presented in Figs. 21-24 show satisfactory degree of convergence with the ones obtained by measurements (Figs. 26-29). Discrepancies between simulation and measurements in the case of pulsation of torque and current are mainly caused by non-sinusoidal shape of the voltage supply which had been used in laboratory test (4% total harmonic distortion) and due to neglecting non-linearity of magnetic circuit in the simulating method.

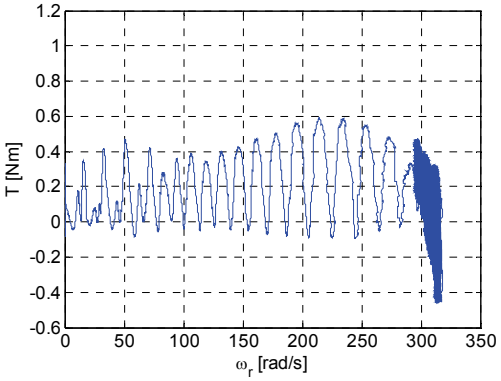

Fig. 26. Measured torque-speed characteristic at rated load for C= 3μF, J=0.00035 kgm^2

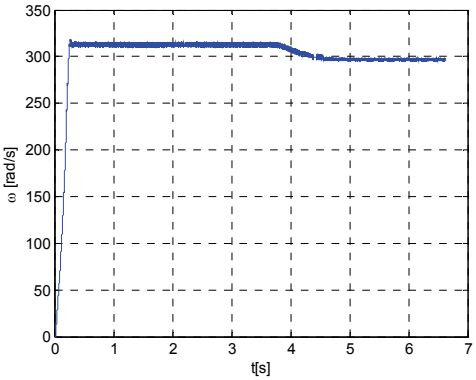

Fig. 27. Measured angular velocity of rotor $\omega_r(t)$ at rated load: C= 3μF, J=0.00021 kgm^2

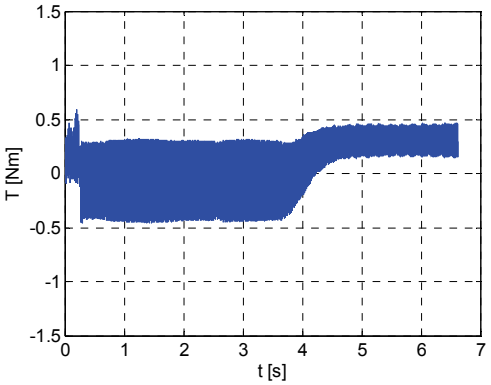

Fig. 28. Measured electromagnetic torque $T_e(t)$ at rated load: C= 3μF, J=0.00021 kgm^2

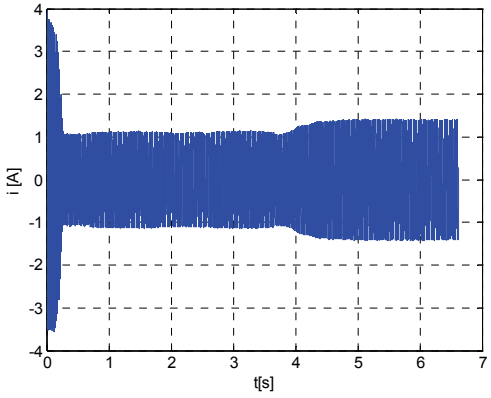

Fig. 29. Measured intake current at rated load: C= 3μF, J=0.00021 kgm^2

Conclusions

Application of the stationary *dq* model of the single-phase capacitor induction motor makes possible simulation of dynamic performance characteristics and selection of the capacitor capacitance to obtain desired starting transients at minimal pulsation of the torque and angular velocity. More accurate simulation of performance characteristics require taking into account of non-linearity of magnetic circuit of the motor and skin-effect in the rotor bars. It needs in turn combining the above circuit method with numerical calculation of the magnetic field in the motor in order to consider changes of inductance and resistance parameters especially at starting of the motor. Despite of its some inaccuracy in simulating dynamic behaviour of the motor the above presented mathematical model is very effective as regards time of computation.

REFERENCES

[1] Fitzgerald A.E., Kingsley C., Jr., Umans S.D., Electric Machinery sixth edition, *McGraw-Hill Companies*, 2003.

[2] Lyshevski S. E., Electromechanical Systems and Devices, *CRC Press*, 2008.

[3] Śliwiński T., Computational methods of induction motors, *PWN*, Warsaw, 2008, Poland. (in Polish)

[4] Tichenor J.L., Chapman P.L., Sudhoff S.D., Budzynski R., *Analysis* of generically gonfigured PSC induction machines, IEEE Transactions on Energy Conversion, Vol. 14, No. 1, March 1999, pp. 108-114.

[5] Cherl-Jin Kim, Chul-Yong Choi, Dal-Eun Lee, Guen-Soo Chi, Soo-Hyun Baek, Torque characteristics of single-phase induction motor for phase control method, *Electrical Machines and Systems, 2003, ICEMS 2003*, Vol. 2, pp. 510-513.

[6] Fei R. W., Lloyd J.D., Dierkes M.C., An experimental study of single-phase induction motor starting performance and its dependency on winding harmonics, *Industry Applications Conference, 1995, IAS'95*, 8-12 Oct 1995, Orlando, FL, 1995, Vol. 1, pp. 571-578.

[7] Williamson S., Smith A.C., A unified approach to the analysis of single-phase induction motors, *IEEE Transactions on Industry Applications*, Jul/Aug 1999, Vol. 35, No. 4, pp. 837-843.

[8] Verma V., Pant P., Singh B., Simulation of a single-phase induction motor with dynamic capacitor for maximum torque operation, *Power System Technology and IEEE Power India Conference, 2008, POWERCON 2008, IEEE Conferences*, 2008, pp.1-6.

[9] Jawad Faiz, Ojaghi M., Keyhani A., PSPICE simulation of single-phase induction motors, *IEEE Transactions on Energy Conversion*, March 1999, Vol. 14, No. 1, pp. 86-92.

[10] Makowski K., An analytical model and parameters of the single-phase capacitor induction motor, *Modelling, Simulation and Control, A, AMSE Press,* Vol. 21, No. 2, 1989, pp. 29-38.

[11] Makowski K., Wilk M., Simulation of dynamic and steady-state operation of the single-phase capacitor induction motor, *Electrical Review*, No. 10, 2009, Poland, pp. 24-28.

[12] Lyshevski S. E., Engineering and Scientific Computations Using MATLAB*, John Wiley &Sons*, *Inc*., 2003.

Authors: *Prof. Krzysztof Makowski, D.Sc., Ph.D., Wroclaw University of Technology, Institute of Electrical Machines, Drives and Measurements, Poland,*
e-mail: krzysztof.makowski@pwr.wroc.pl
Ph.D. student Marcin J. Wilk, M.Sc., Wroclaw University of Technology, Institute of Electrical Machines, Drives and Measurements, Poland,
e-mail: marcin.j.wilk@pwr.wroc.pl